CENTRAL RESEARCH LIBRARY
DOCUMENT COLLECTION

ORNL "Magnetic..."

Magnetic Susceptibility of Germanium

D. K. Stevens, J. W. Cleland, J. H. Crawford, Jr. and
H. C. Schweinler

Oak Ridge National Laboratory
Oak Ridge, Tennessee

Cy. 1

I Introduction

The magnetic susceptibility of conduction electrons in solids has been a subject of interest for many years. The weak, temperature-independent paramagnetism of the simple metals was first explained in terms of the paramagnetism of a degenerate electron gas by Pauli.[1] Somewhat later, Landau[2] showed that, because of quantum effects, free electrons should exhibit an orbital diamagnetism whose magnitude is precisely one-third of their spin paramagnetism. Stoner[3] has given a complete treatment of the combined effects in the case of free electrons. In a solid, Peierls[4] has shown that because of interactions between the conduction electrons and the periodic potential of the crystal, Landau's result holds only when the Bohr magneton is replaced by an effective Bohr magneton which takes account of the interactions in terms of the appropriate effective mass of the charge carriers.[5]

Although much can be learned concerning the band structure of metals from the temperature dependence of their magnetic susceptibility,[6] because their electron gas is essentially completely degenerate, it is virtually impossible to separate experimentally the contribution of the conduction electrons from the total susceptibility in most metals with static magnetic susceptibility measurements. In semiconductors, however, this limitation does not apply. Here statistics governing the behavior of charge carriers range over the domain of classical as well as Fermi-Dirac statistics and the

DO NOT TRANSFER TO ANOTHER PERSON

If you wish someone else to see this document, send in name with document and the library will arrange a loan.

CENTRAL RESEARCH LIBRARY
DOCUMENT COLLECTION

LIBRARY LOAN COPY

magnetic behavior of a classical gas of quasi-free electrons or holes is well understood.[7] Consequently, it is possible in many semiconductors of interest to examine separately the susceptibility of the charge carriers, a property which, as we shall see, provides a significantly new approach to the study of the electronic structure of semiconductors.

The importance of magnetic susceptibility in electronic structure investigations of semiconductors was first recognized by Busch and Mooser.[8] From a systematic study of the susceptibility of gray or α-tin, they were able to determine the forbidden energy gap, the ionization energy of various doping impurities and the effective masses of electrons and holes in this material. The effectiveness of such an approach is brought out even more forcefully when it is remembered that, at the time of their work, α-Sn was available only in the form of powder or pressed compacts. Consequently, the more customary approach involving measurements of electrical conductivity and Hall constant were rendered ineffective because of the interparticle resistance in the compacted specimens. This limitation indicates the unique advantage of magnetic susceptibility measurements in that the carrier susceptibility is essentially independent of transport or scattering processes.

Since the outstanding work of Busch and Mooser, this method of study has been applied to two other diamond-lattice semiconductors: InSb and Ge. Analysis of the magnetic behavior of InSb in both the intrinsic and extrinsic ranges[9] yields a forbidden energy gap of 0.262 ev. in reasonable agreement with the value obtained from electrical measurements,[10] and an electron effective mass of $\sim 0.028\ m_o$.

The magnetic properties of Ge have been investigated by several workers. The first measurements of Ge specimens of known impurity content were made

in 1952 by McGuire[11] over the range from 77 to 300°K. Although his results suffer to some extent from poor sensitivity, they are in qualitative agreement with those reported here. In a preliminary report[12] of the present work, it was shown that the carrier susceptibility χ_c is of sufficient magnitude in both n- and p-type material to make a magnetic investigation worthwhile, and, in addition, an unexplained temperature dependent diamagnetism which can only be attributed to the lattice atoms was observed in high purity specimens. A subsequent analysis[13] of the earlier results gives electron effective masses which are consistent with those obtained from cyclotron resonance experiments.[14,15] Moreover, in the case of n-type Ge, the data suggest that the energy surfaces of the conduction band are best represented by four ellipsoids rather than eight which is the expected result if the minima of the E vs k curves along the [111] direction lie at the boundary of the first Brillouin zone rather than within it.[16] Recently Busch and Helfer[17] have extended the range of measurement to high temperature and, besides observing the onset of the intrinsic process, have noticed a curious hysteresis in the susceptibility on cycling through temperatures in excess of 650°K. They attribute this effect to the thermal introduction of lattice imperfections. In a subsequent paper van Itterbeek et al[18] report susceptibility measurements in the liquid hydrogen range and have observed the recombination of carriers with their parent donor and acceptor centers.

In this paper we wish to summarize the results of a study of the magnetic behavior of a wide variety of Ge specimens. This investigation was motivated by a long-standing study of the effect of fast neutron bombardment on the semiconductivity of Ge.[19] It was hoped that a study of the susceptibility of irradiated specimens would be of value in understanding the nature of the

bombardment induced energy levels. Consequently, in addition to results on unirradiated specimens, we include preliminary information obtained on specimens exposed to fast neutrons. The experimental results have been interpreted in the light of recent ideas concerning the band structure of Ge.

II The Theory of Susceptibility in Germanium

The total susceptibility of a semiconductor may be represented as the sum of three components: The contribution of lattice atoms χ_A, that of the impurity atoms χ_I and the carrier susceptibility χ_c. In the general case each of these components has been treated in detail by Busch and Mooser.[8] Consequently, we shall confine our attention to those points of immediate interest as regards Ge. Our task is to obtain the carrier susceptibility and this requires that there be an accounting for the impurity and lattice contributions.

A. Lattice Susceptibility

The diamagnetism of an assembly of atoms is usually expected to be rather small ($< 10^{-6}$ emu/g) and essentially temperature independent.[20] Theory is applicable, however, only to spherical, closed-shell atoms, the resultant diamagnetic susceptibility of a solid being taken as the sum of the atomic contributions. In diamond lattice structures, the covalent binding is produced by the sp^3 hybridized orbitals of the valence electrons and, because of the directional nature of such bonds, the usual assumptions no longer hold. It is expected, however, that the contribution of the cores can be obtained in good approximation by such an approach. We have computed the susceptibility of the Ge^{4+} ion from the Hartree functions[21] and the customary relation

$$\chi_{ion} = \frac{N z_1 e^2 \overline{r^2}}{6 m c^2} \qquad (1)$$

where N is the number of ions per gram of Ge, z_i is the number of electrons per ion and $\overline{r^2}$ is the average of the radii squared. The value obtained is $\chi_{ion} = 1.265 \times 10^{-7}$ emu/g. This value would be reduced somewhat if Hartree-Fock functions were used, but these unfortunately are not available. As we shall show, this value is greater than that observed for the total diamagnetism for a pure specimen, the latter including the effect of the valence electrons as well. Moreover, the observed χ_A is appreciably temperature dependent. The reason for this curious behavior is not yet understood. Consequently, we rely entirely on experiment for the value of χ_A.

B. The Carrier Susceptibility

The results obtained for the susceptibility of a perfect electron gas, modified appropriately for the periodic potential of the lattice, may be applied directly to conduction electrons.[5] Neglecting higher order terms in magnetic field, the specific susceptibility for electrons is

$$\chi_c = (\beta^2/3\rho k)\, \omega_e\, C\, M_e^{(N)3/2}\, T^{1/2}(3-\overline{f_e^2})\, F'_{1/2}(\eta) \qquad (2)$$

where β is the Bohr magneton, ρ is the density of Ge, ω_e is the statistical weight or degeneracy of states (exclusive of spin) in the conduction band, $C = \left[4\pi\,(2\,m_o\,k)^{3/2}\right]/h^3$, $M_e^{(N)}$ is the effective mass ratio for the density of states expression ($M = m^*/m_o$) and $\overline{f_e^2}$ is the appropriate value of the square of the reciprocal mass ratio tensor for orbital motion of the electrons in the magnetic field. The function $F'_{1/2}(\eta)$, where $\eta = \zeta/kT$, is the first derivative of the Fermi integral

$$F_{1/2}(\eta) = \int_0^\infty x^{1/2}\left[1 + e^{x-\eta}\right]^{-1} dx \qquad (3)$$

The values of $F_{1/2}(\eta)$ and, by means of the tabulated functions,[22] $F'_{1/2}(\eta)$ may be obtained from the electron concentration n and the relation

$$n = \omega_e C(M_e^{(N)}T)^{3/2} F_{1/2}(\eta) \tag{4}$$

For sufficiently high temperatures or low carrier concentrations ($\eta < -3$) classical statistics apply. Under these conditions Eq. (2) becomes

$$\chi_c = (\beta^2/3\rho kT)\, n\, (3-\overline{f_e^2}) \tag{5}$$

from which it is evident that the slope of the χ_c vs 1/T curve is proportional to $(3-\overline{f_e^2})$. Since n is readily obtained from Hall coefficient measurements, $\overline{f_e^2}$ may be obtained from Eq. (5) in the classical range. Although we have treated conduction electrons only, analogous expressions apply to holes in the valence band. Since the extrinsic range is the only one of interest here, we shall not treat the carrier susceptibility in the intrinsic range.[22]

The values of effective mass ratios appropriate to the density of states ($M_e^{(N)}$) and orbital motion $\left[M_e^{(M)} = (\overline{f_e^2})^{-1/2}\right]$ depend on the curvature of energy surfaces in k-space. Cyclotron resonance experiments[14,15] have firmly established that for the conduction band of Ge the energy surfaces can be represented by ellipsoids of revolution whose major axes lie along the [111] k directions. Hence, the energy surfaces are described in terms of two mass parameters, M_t and M_l which are the transverse and longitudinal effective mass ratios respectively. The values of the effective mass ratios may be obtained conveniently by a transformation of coordinates. In the case of $M_e^{(N)}$ a transformation of the momentum coordinates with respect to each minimum into an isotropic coordinate frame results in the introduction of the factor $\omega_e \sqrt{M_t^2 M_l}$ into the expression for the classical partition function. ω_e is equal to the number of complete minima[16] and takes a value of eight if the minima lie within the first Brillouin zone or a value of four if they lie

at zone boundary. Hence $M_e^{(N)} = (M_t^2 M_l)^{1/3}$.

The method of averaging used for $\overline{f_e^2}$ is somewhat more complex. Here, a similar transformation of momentum coordinates made in the expression for energy in the presence of a magnetic field requires a further transformation of the magnetic field components. When the details of the computation are carried through, the appropriate combination of principal mass ratios turns out to be

$$\overline{f_e^2} = (2 M_t + M_l)/3 M_t^2 M_l.$$

Using now the reported values for the principal masses[14,15] ($M_t = 0.083$ and $M_l = 1.4$), we obtain $M_e^{(N)} = 0.216$ and $\overline{f_e^2} = 54.1$. If in addition we use $\omega_e = 4$, as indicated by an analysis of the temperature dependence of the susceptibility of n-type Ge,[13] Eqs. (2) and (4) may be written

$$\chi_c = 4.26 \times 10^{-9} T^{1/2} F'_{1/2}(\eta) \tag{2a}$$

$$n = 2.12 \times 10^{15} T^{3/2} F_{1/2}(\eta) \tag{4a}$$

The calculations of Kittel et al[14] and Herman[24] indicate that the valence band is composed of three doubly degenerate, nonspherical bands and is therefore somewhat more complex than the conduction band. The maximum of these bands appears to fall at $\underline{k} = 0$, two of them coinciding at that point to form the valence band edge. Because of spin-orbit interactions the third band which is nearly spherical lies below the other two by the interaction energy ΔE. In order to evaluate the effective mass parameters of Eq. (2), it is necessary to use the energy expressions for these bands which, to a good approximation for Ge, are given by Kittel et al[14] in terms of three curvature parameters. The value of $M_h^{(N)}$ is obtained directly from the classical partition function which can be summed rigorously using the energy

expressions. Such a sum for the two upper bands leads directly to the double integral

$$M_{1,2}^{3/2} = 1/4\pi \iint \frac{d\Omega}{\left\{A \pm \sqrt{B^2 + C^2 g(\vartheta, \varphi)}\right\}^{3/2}} \tag{6}$$

where the subscripts 1 and 2 and the upper and lower signs in the integral refer to the "light" and "heavy" bands respectively, the curvature parameters are identical to those of Kittel et al[14] except for the factor ($\hbar^2/2\, m_o$), and

$$g(\vartheta, \varphi) = \sin^4 \vartheta \cos^2 \varphi \sin^2 \varphi + \sin^2 \vartheta \cos^2 \vartheta \tag{7}$$

The lower band (Band 3) gives

$$M_3^{3/2} = A^{-3/2} \tag{8}$$

Numerical integration of Eq. (6) using the appropriate values of the curvature parameters yields $M^{3/2}$ values of 0.0091, 0.199, and 0.0213 for bands 1, 2, and 3 respectively. Hence

$$M_h^{(N)3/2} = 0.208 + 0.0213\, e^{-\Delta E/kT} \tag{9}$$

The orbital effective mass presents additional difficulties and a rigorous treatment requires an approach for each band similar to that used for electrons. However, it was observed in the integration of Eq. (6) that the corrections for lack of sphericity were small even for the most nonspherical band (Band 2). Consequently, we use an approximate approach in which the error is probably not greater than 5%. To a good approximation, even in the magnetic field,

$$M_{1,2}^{-1/2} = 1/4\pi \iint \left\{A \pm \sqrt{B^2 + C^2 g(\vartheta, \varphi)}\right\}^{1/2} d\Omega. \tag{10}$$

Integration leads to $M_h^{-1/2}$ values of 4.80, 1.74, and 3.605 for Bands 1, 2, and 3 respectively. Hence

$$\overline{f_h^2} = M_h^{-1/2}/M_h^{3/2} \cong 31.4 + 14.1\, e^{-\Delta E/kT} \tag{11}$$

Consequently, both $M_h^{(N)}$ and $\overline{f_h^2}$ are temperature dependent through the Boltzmann factor containing the spin-orbit splitting energy. Optical absorption of holes in Ge suggests[25] that $\Delta E \sim 0.3$ ev. If such is the case, the mass parameters are expected to be essentially temperature independent in the temperature range used here and $M_h^{(N)3/2} = 0.208$ and $\overline{f_h^2} = 31.4$. A similar calculation using the slightly different curvature parameters of Lax et al[15] gives almost identical values.

C. The Impurity Contribution

In the specimens used here we are interested only in the usual acceptor and donor doping impurities of the third and fifth columns of the periodic system. Since these impurity atoms presumably fit substitutionally into the semiconductor lattice, they may be treated as hydrogen-like systems to an approximation sufficiently good for this purpose. Busch and Mooser,[8] have examined this case in detail both for the low concentration limit in which the impurity atoms may be treated independently and for concentrations sufficiently high that the impurity wave-functions overlap and form degenerate impurity bands. Because of their substitutional arrangement, one expects an appreciable contribution only when they are un-ionized. Besides the paramagnetic term associated with the unpaired electron-spin, these authors show that for a large dielectric constant the electron or hole orbit is of such a size that an appreciable diamagnetic term may also exist in the small concentration case. Using the numerical constants appropriate for Ge, the low concentration limit gives

$$\chi_I = N_I^o \left[1.17 \times 10^{-25}\, T^{-1} - 3.4 \times 10^{-28}\right] \qquad (12)$$

where N_I^o is the concentration of un-ionized impurities of the type in question. In obtaining the diamagnetic term it is assumed that the effective mass of

the bound carrier is equal to the electronic mass and germanium has a dielectric constant of 16.1. In the case of impurity bands, equations analogous to Eq. (2) are obtained which contain the effective mass ratios appropriate to the impurity band. There is no way available at present for evaluating these mass ratios.

In nearly all specimens used here the ionization energies are so small that the impurities are essentially completely ionized over the entire temperature range (70 to 300°K). Therefore, the impurity contribution discussed above is not of immediate interest. For the irradiated specimens, however, an estimate of the contribution of the trapped carriers is important. In order to do this, a model of the bombardment introduced defects is necessary and the only one available at present which is to any extent justified is that proposed by James and Lark-Horovitz.[26] This model, which has been tested experimentally,[19] requires that each interstitial and each vacancy be responsible for two localized states in the forbidden band. When these defects are present in equal concentration there are two vacant states capable of trapping conduction electrons in n-type Ge: one which lies below the middle of the forbidden band and is therefore capable of acting as an acceptor in p-type Ge and another much more shallow one which has been experimentally located at 0.2 ev. below the conduction band. On irradiating n-type Ge with a high initial electron concentration n^o, both levels are to some extent occupied until the concentration of defect pairs becomes equal to one-half n^o. Further irradiation favors population of the lower acceptor state until all electrons are trapped therein and conversion to p-type occurs. Therefore, at the minimum conductivity, essentially all of the electrons are trapped in a state that has been tentatively identified as one corresponding to a singly ionized interstitial atom. If the defects are randomly

distributed and their associated wave functions do not overlap appreciably, a paramagnetic contribution equal to that for n_o free spins should result. The diamagnetic contribution depends on the radial extent of the wave functions of the trapped electron. Since the interstitial ion has a residual charge, the electron orbit will be considerably decreased over that estimated above for a hydrogen-like impurity and the diamagnetic contribution is expected to be quite small. Should the defect functions overlap, a paramagnetic contribution of much smaller magnitude and temperature dependence would result. Such a condition may exist even for relatively short irradiations if the defects are highly localized in the region of the primary (fast neutron) collision.

In this picture the vacancy should be occupied by two electrons at the conductivity minimum. Here the diamagnetic contribution might be appreciable. Both the coulombic repulsion of the electrons and their relatively loose binding (they presumably fill two of the four half-filled orbitals extending into the vacancy) would tend to produce a large orbit. Unfortunately, it is not possible to make a quantitative estimate of their contribution on the basis of present knowledge.

III Experimental

The magnetic susceptibilities of single crystal cubes having edge lengths of approximately 5 mm were measured by the Faraday technique using a balance similar to that of McGuire and Lane.[27] In order to increase the balance sensitivity the photo-tube optical system was replaced by a linear differential transformer and the beam suspension was fabricated out of Elgiloy rather than nichrome or phosphor bronze. The sample cubes were suspended from the balance on 0.001" diameter molybdenum wire into the fringing field of an Arthur D. Little

electromagnet, the field of which could be controlled and reproduced to approximately ±.01%. Sample temperatures were taken as those of the walls of the copper sample tube adjacent to the specimen, helium at a pressure of 125 microns of Hg being used as an heat exchange medium.

The absolute value of the room temperature susceptibility of each sample was measured using oxygen at a known pressure and temperature as a calibrating agent. The force exerted on a body of volume v and volume susceptibility $\mathcal{X}$ suspended in an inhomogeneous field H is given by

$$F_o = \left[\frac{(\mathcal{X} - \mathcal{X}_o)}{2}\right] v \nabla H^2 \tag{10}$$

where $\mathcal{X}_o$ is the volume susceptibility of the surrounding medium and ∇H^2 is the gradient of the field squared at the sample. The susceptibility of an irregularly shaped body is given by the expression

$$\mathcal{X} = \left[\frac{F_v}{F_v - F_o}\right] \mathcal{X}_o \tag{11}$$

where F_v is the force experience by the body when suspended in a vacuum and F_o is the force experienced when suspended in a medium having a susceptibility $\mathcal{X}_o$.

In this work F_v was measured at four values of the field ranging from 12 to 20 kilo-oersteds. Oxygen was then admitted to the system, the measurements repeated at the same field settings, and $\mathcal{X}$ calculated for each field value. A systematic trend of $\mathcal{X}$ with field was considered an indication of ferromagnetic contamination and the sample was recleaned. Otherwise, the calculated values were averaged to obtain the absolute value of the room temperature susceptibility of each sample. Using this technique the absolute accuracy of this point is ±0.6%. The susceptibilities at other temperatures were determined relative to this room temperature point with a precision of

$\pm 0.1\%$.

Carrier concentrations were obtained from Hall coefficient and conductivity measurements obtained on control specimens which were cut from the original ingot adjacent to the susceptibility cube. In several cases, when inhomogeneity in the impurity distribution was suspected, Hall plates were prepared from successive ingot slices cut radial to the cube and perpendicular to the direction of growth. The average concentration obtained on these plates was used.

One cube, together with its control specimen, was given successive exposures to fast neutrons in a fission chamber in the Oak Ridge Graphite reactor. The irradiations were carried out at $\sim 30^{\circ}C$ and susceptibility and Hall coefficient measurements were made after each exposure.

IV Results

A. High Purity Germanium

For extrinsic carrier concentration $< 10^{16}$ cm^{-3}, χ_c is below the limit of detection in the temperature range employed. Consequently, values of χ obtained on high purity specimens should yield χ_A for Ge directly. The temperature dependence of χ for two n-type specimens ($n = 1 \times 10^{13}$ cm^{-3} and 1×10^{14} cm^{-3}) are shown in Fig. 1. Because of the absolute precision from one curve to the other of only $\pm 0.6\%$, the curves were adjusted to correspondence at $150^{\circ}K$. As expected, the points for both specimens fall essentially on the same line.

As mentioned above, the atomic diamagnetism is expected to be only slightly temperature dependent. In contrast, the curves of Fig. 1 exhibit a very appreciable temperature variation. Normally a relative increase of

diamagnetism of the same order as the cubical expansion coefficient might be expected. For Ge, however, the dependence is in the opposite direction and the relative change is an order of magnitude greater than the expansion coefficient ($d \log \chi/dT = 2.3 \times 10^{-4}$ at $300^{\circ}K$). Although we assume that the nature of the binding in the diamond-lattice is responsible, the reason for this curious behavior is not yet known. In order to investigate this point further, a specimen of high purity silicon ($n \sim 10^{14}$ cm^{-3}) and a gem quality diamond were examined. The silicon specimen gave a χ vs T curve which is quite similar to that of Ge while for the diamond χ is temperature independent within experimental error ($\pm 0.1\%$) in this temperature range.

B. N-type Germanium

The diamagnetic susceptibility vs temperature curves for a number of n-type Ge specimens of known electron concentration are shown in Fig. 2. Also shown for comparison is the curve for a high purity, zone refined n-type specimen ($n < 10^{14}$ cm^{-3}). In every case except the latter the contribution of the extrinsic electrons is evident.

The values of χ_c are obtained for each specimen by subtracting, point by point, the susceptibility of the high purity specimen. The resulting values for three of the specimens is shown in Fig. 3 in the form of $-\chi_c$ vs 1/T curves. The curves are essentially linear in the high temperature range as predicted by Eq. (5). Toward lower temperature the curves begin to fall off indicating a transition from classical to Fermi-Dirac statistics. In Table I we have summarized the data on n-type Ge. The second column lists the high temperature (low 1/T) linear slope. The third column lists the values of n obtained on comparison Hall specimens appropriately corrected for impurity scattering[28] and carrier degeneracy.[29] After such corrections the values of n were found

TABLE I

Summary of results obtained on n-type Ge. The sample numbers correspond to the numbers on the curves of Figs. 2 and 3. Columns 2, 3 and 4 list the slopes of the χ_c vs 1/T curves in the classical (linear) region, the electron concentrations and the values of $\overline{f_e^2}$ respectively.

Sample	$-\left[d\chi_c/d(1/T)\right]_{cl}$	n[a]	$\overline{f_e^2}$
1[b]	4.85×10^{-8}	3.1×10^{16}	~43
2	1.46×10^{-6}	7.5×10^{17}	52.6
3	1.45×10^{-6}	1.3×10^{18}	31.6
4	4.57×10^{-6}	5.0×10^{18}	26.4
5	5.59×10^{-6}	1.3×10^{19}	14.0

[a] Values of n were obtained from the Hall coefficient and conductivity curves as a function of temperature, corrections for impurity scattering and, where necessary, carrier degeneracy being made (references 28 and 29).

[b] The electron concentration of this specimen was appreciably temperature dependent. Therefore, the observed value of $\overline{f_e^2}$ might be expected to be somewhat smaller than its true one.

to be temperature independent over the entire range to $\sim 5\%$ with the exception of sample 1. In the fourth column we list the values of $\overline{f_e^2}$ obtained from the slope and values of n. These values are accurate to about 15%.

It is interesting to note that for the purer specimens agreement of $\overline{f_e^2}$ with the expected value of 54 is quite reasonable, while with increasing donor concentration the value of $\overline{f_e^2}$ decreases markedly. Herring[30] has pointed out that the presence of an impurity band which is expected to overlap the conduction band at high donor concentrations would be expected to change the effective mass of the carriers when the overlap becomes appreciable.

Except for sample 1 of Table I, the χ_c vs 1/T curves of the n-type specimens depart from linearity toward the higher 1/T values, exhibiting a downward concavity. In the case of samples 2 and 3 this curvature can be accounted for quite adequately on the basis of transition from classical to Fermi-Dirac statistics provided $\omega_e = 4$ rather than 8. With this value of ω_e, Eq. (2) yields an acceptable fit to the data over the entire temperature range. The results of this analysis have already been reported[13] and these have been taken as evidence that the minima of the E vs k surfaces lie on or within kT of the zone boundary. Attempts to fit the more impure specimens (4 and 5 of Table I) within the framework of the cyclotron resonance results were not successful nor could a suitable correlation be obtained by using Eq. (2) and the experimental values of $\overline{f_e^2}$ while treating $M_e^{(N)}$ as an adjustable parameter. The experimental curves fall off more rapidly at low temperature than those calculated, in a manner which suggests that the effective mass decreases with increasing 1/T. In view of the postulated effect of an overlapping donor band mentioned above, this behavior is not surprising since,

for a mixture of conduction states the average effective mass might well depend on the position of the Fermi level.

It is of course possible that impurity band overlap might also explain the curvature toward low temperature of samples 2 and 3 which has been attributed to carrier degeneracy. In fact Debye and Conwell[31] have examined the dependence of donor ionization energy on donor concentration in n-type Ge and, within the limitations of necessary assumptions, have shown that the ionization energy becomes zero for net donor concentrations in the neighborhood of 1.5×10^{17} cm^{-3}. If the ionization energy can be taken as an index of band overlap, this would indicate that a mixing of donor and conduction states might also occur in samples 2 and 3. In this regard, Johnson and Shipley[32] have made a careful analysis of the temperature dependence of the Hall coefficient of a specimen containing a net donor concentration of 2.16×10^{18} cm^{-3} and they find an ionization energy of -0.005 ev. Hence the ionization energies of the specimens in question are expected to lie closer to the band edge than 0.005 ev. For the temperature range in question, since effects of carrier degeneracy are not excessive, we expect the donor states to exert only a small influence on the effective mass of conduction electrons for these specimens. In further support of the choice of $\omega_e = 4$, Debye and Conwell find that an average effective mass ratio between 0.2 and 0.5 gives the most consistent fit to all their data. The average effective mass ratio arising from the density of states expression is $M_e^* = M_e^{(N)}(\omega_e)^{2/3}$. This gives average mass ratios of 0.51 and 0.85 for ω_e values of 4 and 8 respectively. In order to establish the value of ω_e conclusively, it is necessary to examine the behavior of χ_c on a higher purity sample ($n \simeq 10^{17}$ cm^{-3}) in the range of lower temperatures.

C. P-Type Germanium

Measurements similar to those on n-type material have been carried out on several p-type samples. The temperature dependence of diamagnetism is shown in Fig. 4 and the $-\chi_c$ vs 1/T curves in Fig. 5 for representative specimens. The data are summarized in Table II. The values of $\overline{f_h^2}$ with one exception (sample 2) are considerably smaller than the value of 31.4 indicated by cyclotron resonance. Again, as for n-type material, this departure from expectation apparently increases with increasing acceptor concentration. Since the deviation seems to set in at a much lower carrier concentration than in n-type material, it is possible that the critical acceptor concentration required for the formation of an overlapping impurity band is smaller than for donors. However, even for 8×10^{16} acceptors cm^{-3} (sample 1 of Table II) the $\overline{f_h^2}$ is only ~ 20 and for such a small acceptor concentration an overlapping band does not appear likely. Consequently, we conclude that the discrepancy between observed and expected $\overline{f_h^2}$ values is real. The reason for the lack of agreement is unknown. It is possible that the energy surface curvatures in the valence band are sufficiently complex that the cyclotron resonance results obtained at 4^oK are no longer applicable in this temperature range. In this connection, it is noteworthy that a detailed analysis of the field dependence of the p-type Ge Hall coefficient,[33] although in agreement with the general features of the valence band as revealed by cyclotron resonance, also fails to give a quantitative correlation. The results of this analysis indicate that the fraction of holes in Band 1 is only 0.02 of the total whereas the ratio of effective masses indicates a value of 0.045. A smaller than expected population of Band 1 would also explain the deviation reported here.

TABLE II

Summary of results obtained on p-type specimens. The sample numbers correspond to those given on the curves of Figs. 4 and 5. Columns 2, 3 and 4 list the classical slopes of the χ_c vs 1/T curves, the hole concentrations, and the values of $\overline{f_h^2}$ respectively.

Sample	$\left[d\,\chi_c/d\,1/T\right]_{cl}$	p^a	$\overline{f_h^2}$
1	5.2×10^{-8}	7.8×10^{16}	20
2	1.7×10^{-7}	1.9×10^{17}	26
3	2.8×10^{-7}	4.4×10^{17}	18
4	3.2×10^{-7}	5.1×10^{17}	20
5	2.9×10^{-7}	5.4×10^{17}	18
6	2.0×10^{-6}	5.3×10^{18}	12

[a] Although impurity scattering and carrier degeneracy corrections were made in obtaining these values, the magnetic field dependence of Hall coefficient, which is known to be appreciable in p-type Ge (reference 31), was not accounted for explicitly. The error involved, however, should not be large.

Attempts to fit the χ_c vs 1/T curves of Fig. 5 for samples 1, 2, and 3 of Table II according to Eq. (2) with experimental carrier masses reveal that there is a significant concave downward curvature toward high 1/T values which is too great to be explained by either transition to Fermi-Dirac statistics, higher order terms in H in the susceptibility equation, or a combination of these. Since analysis of Hall coefficient and resistivity data for these specimens indicates that the hole concentrations are essentially constant over the temperature range in question, it appears that $\overline{f_h^2}$ decreases to some extent with decreasing temperature. Although the contribution to $\overline{f_h^2}$ of the third valence band is temperature dependent through a Boltzmann factor containing the spin-orbit splitting energy, it was indicated above that this is not expected to introduce appreciable temperature dependence in this temperature range because of the large value that has been indicated for ΔE.

D. Bombarded Germanium

The effect of fast neutron bombardment on the magnetic susceptibility was investigated on one n-type specimen (sample 2 of Table I). The susceptibility was measured as a function of temperature after each successive exposure and representative results are shown in Fig. 6. The combined carrier and impurity (defect) susceptibilities were obtained by subtracting the values of a pure specimen at each temperature and this, designated as $\Delta\chi$, is plotted against 1/T in Fig. 7. The data are summarized in Table III. Column 1 lists the integrated fast neutron flux, Column 2 the linear slope, the electron concentrations obtained from an analysis of the Hall coefficient and resistivity is given in Column 3 and in Column 4 the values of $\overline{f_e^2}$ obtained from the slopes are given. The reciprocal mass ratio is in good agreement with the expected value of 54 and the scatter gives a good indication of experimental error.

Also shown in Table III are the values of n calculated from the slopes assuming $\overline{r_e^2} = 54$. The variation of n with exposure is compared with the conductivity σ in Fig. 8. Values of n obtained by the two methods (Columns 3 and 5) show a variation with exposure which is quite similar to that of σ.

Examination of the χ vs 1/T curves obtained after long exposure (not shown in Fig. 7) reveals that, although the curves are quite linear at low temperature, there is a marked upward concavity at high temperatures (low 1/T). This behavior may or may not be real. Although it is possible that exposure has decreased the temperature dependence of χ_A in the high temperature region, thus introducing an apparent curvature into the $\Delta\chi$ vs 1/T curves, this behavior may also be explained as being caused by a variation of the sample suspension length with temperature. The thermal expansion of molybdenum, though small, is sufficient between room and dry ice temperatures to move the specimen into a lower region of H $^{dH}/_{dz}$ provided the position at room temperature were at the maximum field square gradient. More careful measurements are necessary before this effect can be interpreted. In any event, since molybdenum is a high temperature metal, its expansion coefficient is quite small below 200°K and the temperature dependence of $\Delta\chi$ in this range (70 to 200°K) should be valid.

It is interesting to note that there is no indication of the temperature dependent paramagnetism expected to result from unpaired electrons. In Fig. 9 we compare the χ vs T curves for a pure specimen (curve 0) and the two longest exposures (curves I and II) for which essentially all electrons have been trapped. For clarity, Curve 0 has been displaced downward by 0.7% in order to avoid congestion. Also shown (Curve 0', dashed) is the expected χ vs T curve relative to Curve 0 for a specimen containing 7.5×10^{17} unpaired

TABLE III

Summary of results obtained on n-type specimen (sample 2 or Table I) irradiated with fast neutrons. The integrated fluxes are listed in column 1. Columns 2, 3 and 4 list the classical slopes, the electron concentrations, and f_e^2 values respectively. Column 5 gives the values electron concentration n_M caluclated from the classical slope assuming $\overline{f_e^2} = 54$.

Exposure Neutrons/cm^2 x 10^{-17}	$-\left[d\Delta\chi/d\ 1/T\right]$	n cm^{-3} x 10^{-17}	$\overline{f_e^2}$	n_M cm^{-3} x 10^{-17}
.72	1.13 x 10^{-6}	5.17	59.0	5.68
1.27	5.33 x 10^{-7}	2.72	53.0	2.68
1.61	2.28 x 10^{-7}	1.33	47.0	1.15
1.84	1.57 x 10^{-7}	.85	50.4	.79
2.07	1.25 x 10^{-7}	.81	42.5	.63
2.30	8.0 x 10^{-8}	.45	48.5	.40
3.00	1.1 x 10^{-8}	----	----	.06

spins per cm^3. It is clearly evident that such a paramagnetic term is not present in the irradiated specimens. This is taken as evidence that the levels responsible for removing electrons are so dense that they have broadened into degenerate bands. At a concentration of 7.5×10^{17} this does not appear too likely, especially in view of considerations concerning the singly ionized interstitial atom as discussed above. Consequently, we tentatively conclude that the defects are not randomly distributed but rather are to a large extent localized in the region of the primary collision of the fast neutron. The latter situation would produce localized regions of high defect-level density which could be described effectively in terms of degenerate impurity bands. In order to establish this point to any degree of certainty it is necessary to examine lower concentrations of trapped electrons. This can be done quite effectively by extending the range of measurement to liquid helium temperatures. Apparatus is being constructed to this end.

V Summary

The results have revealed a number of points of interest regarding the magnetic behavior of Ge. The first and most unexpected of these is the temperature dependence of the susceptibility of high purity specimens. That this is a common property of semiconductors of the diamond-lattice type is suggested by a similar behavior of Si and an indication of such in InSb.[9] It should be noticed, however, that diamond itself has a temperature independent susceptibility. In view of its existence in the lower melting members of the group (both elements and compounds), it would be worthwhile to re-evaluate the results obtained on α-Sn in the light of such a behavior.

The magnetic behavior of n-type Ge is consistent with expectation based on results of cyclotron resonance. The appropriate averages of electron mass

ratios are in reasonable agreement with those obtained by the Berkeley[14] and Lincoln Laboratory[15] groups for the smaller values of n. At the large n-values the effective masses increase markedly which is probably due to a degenerate donor band which overlaps the bottom of the conduction band. Fitting the data to theory in the range of transition from classical to Fermi-Dirac statics suggests that the energy surfaces of the conduction band are represented by four rather than eight ellipsoids of revolution in k-space.

In p-type Ge, agreement with cyclotron resonance experiments is not as convincing. We find that generally the values of $\overline{f_h^2}$ are smaller by at least 30% than the predicted one. The results of a detailed analysis of the Hall coefficient field dependence in p-type Ge yields results which, also fail to yield quantitative agreement.[33] It is possible that the complex band shapes yield different effective mass ratios at temperatures appreciably above the temperature of liquid helium at which the cyclotron resonance measurements were made. A temperature dependent effective mass is to be expected because of the lowering of Band 3 by spin-orbit coupling. However, if the energy lowering is $\sim$0.3 ev as is indicated by optical absorption data, such a temperature dependence would be negligibly small. It is interesting to note in this connection that an examination of hole mobility[34] also indicates a variance between theory an experiment which could be explained if the effective mass were temperature dependent. A more careful study of the hole susceptibility particularly at lower temperature is necessary to clear up this matter.

Studies of fast neutron bombarded Ge reflect only the decrease of electron concentration and reveal no spin paramagnetism which would be expected if the electrons were trapped unpaired in localized states. This behavior is interpreted as indicative of localized fluctuations in the density of fast

neutron introduced lattice defects.

We are deeply indebted to Miss Louise Roth of Purdue University and to D. C. S. Fuller of the Bell Telephone Laboratories who furnished the single crystals of Ge and Si used in these studies. Our thanks also to Mr. Chapman of Kimball's Jewelry, Knoxville, Tennessee, for making available to us the excellent diamond specimen, and Mr. T. R. Green of the Elgin National Watch Company who supplied us with an unheattreated main-spring blank used in the construction of the balance. We finally wish to thank Messrs. J. C. Pigg, Glenn Craig, and W. T. Adams of this laboratory for their invaluable assistance with instrumentation problems and Professor R. L. Sproull of Cornell University for many valuable discussions and suggestions. One of us, (D.K.S.) wishes to express his appreciation to Dr. H. D. Crockford of the University of North Carolina who, in the capacity of faculty advisor, gave freely of his time and energy in coming to Oak Ridge for consultations concerning much of the early work connected with this problem.

FIGURE CAPTIONS

Figure 1: The diamagnetic susceptibility of two high purity germanium specimens as a function of temperature. For comparison, the curves are adjusted to correspondence at 150°K.

Figure 2: The diamagnetic susceptibility vs temperature curves of four n-type germanium specimens. Curve 0 is that for high purity germanium while the numbers of the other curves correspond to the sample numbers of Table I.

Figure 3: The carrier diamagnetism vs reciprocal temperature for n-type germanium. The curve numbers refer to the samples numbers listed in Table I.

Figure 4: The diamagnetic susceptibility vs temperature curves of three p-type specimens and one high purity n-type specimen, curve 0, of germanium. The numbers of the other curves correspond to the sample numbers of Table II.

Figure 5: The carrier diamagnetism vs reciprocal temperature for p-type germanium. The numbers refer to the sample numbers listed in Table II.

Figure 6: The diamagnetic susceptibility vs temperature of a fast neutron bombarded n-type germanium specimen listed as sample 2 in Table I. The exposures are indicated on the curves. The curve of a pure specimen is shown for comparison.

Figure 7: The carrier plus defect susceptibility vs temperature of the fast neutron bombarded germanium sample after the indicated exposures.

Figure 8: The electron concentration and conductivity vs integrated fast neutron flux of the bombarded specimen.

Figure 9: The diamagnetic susceptibility vs temperature of the bombarded specimen after irradiation into the intrinsic region. Curve 1 is for the specimen with approximately 5×10^{15} electrons per cm^3 remaining in the conduction band at $300^{\circ}K$. Curve 2 is after the specimen has become p-type and has less than 10^{15} carriers per cm^3 at $300^{\circ}K$. Curve 0 is for a pure specimen, displaced downward by 0.7% for clarity. Curve 0' is curve 0 to which has been added the expected paramagnetic contribution of 7.5×10^{17} unpaired spins per cm^3.

REFERENCES

1 W. Pauli, Z. Physik 41, 81 (1927).

2 L. Landau, Z. Physik 64, 629 (1930).

3 E. C. Stoner, Proc. Roy. Soc. 152, 672 (1935).

4 R. Peierls, Z. Physik 80, 763 (1933); 81, 186 (1933).

5 H. Frohlich, Theorie der Metalle, Julius Springer, Berlin (1937), pp 144-156.

6 C. J. Kriessman, Revs. Modern Phys. 25, 122 (1953); C. J. Kriessman and H. B. Cullen, Phys. Rev. 94, 837 (1954).

7 See for example R. H. Fowler, Statistical Mechanics, Cambridge University Press (1937), Chapter XII.

8 G. Busch and E. Mooser, Z. Physik Chemie 198, 23 (1951); Helv. Phy. Acta 26, 611 (1953).

9 D. K. Stevens and J. H. Crawford, Phys. Rev. (to be pub. July 15).

10 M. Tanenbaum and J. P. Maita, Phys. Rev. 91, 1009 (1953); Breckenridge et al, Phys. Rev. 96, 571 (1954).

11 T. R. McGuire, unpublished data

12 D. K. Stevens and J. H. Crawford, Jr. Phys. Rev. 92, 1065 (1953).

13 Crawford, Schweinler, Stevens, (submitted to Phys. Rev.).

14 Dresselhaus, Kip and Kittel, Phys. Rev. 92, 827 (1953); Phys. Rev. 95, 568 (1954); Phys. Rev. 98, 368 (1955).

15 Lax, Zeiger, Dexter and Rosenblum, Phys. Rev. 93, 1418 (1954); Dexter, Zeiger, and Lax, Phys. Rev. 95, 557 (1954); Lax, Zeiger, and Dexter, Physica 20, 818 (1954).

16 C. Kittel, Physica 20, 829 (1954).

17 G. Busch and N. Helfer, Helv. Phys. Acta 27, 201 (1954).

18 van Itterbeek, de Greve and Duchateau, Appl. Sci. Res. B 4, 300 (1955).

19 Cleland, Crawford, Lark-Horovitz, Pigg and Young, Phys. Rev. 83, 312 (1951). Cleland, Crawford, and Pigg, Phys. Rev. (To be published).

20 See for example - P. W. Selwood Magneto Chemistry, Interscience Publishers (1943) New York, Chapter II.

21 Hartree, Hartree, and Manning, Phys. Rev. 59, 306 (1941).

22 J. McDougall and E. C. Stoner, Phil. Trans. Roy. Soc. A. 237, 67 (1936).

23 For a treatment of the intrinsic range see references 8, 9, and 17.

24 F. Herman, Physica 20, 801 (1954).

25 A. Kahn, Phys. Rev. 97, 1647 (1955).

26 H. M. James and K. Lark-Horovitz, Z. Physik Chemie. 198, 107 (1951).

27 T. R. McGuire and C. T. Lane, Rev. Sci. Instr. 20, 489 (1949).

28 V. A. Johnson and K. Lark-Horovitz, Phys. Rev. 82, 977 (1951).

29 V. A. Johnson and F. M. Shipley, Phys. Rev. 90, 523 (1953).

30 C. Herring (private communication).

31 P. P. Debye and E. M. Conwell, Phys. Rev. 93, 693 (1954).

32 V. A. Johnson and F. M. Shipley, "A diabatic Hall Effect in Semiconductors," Report of the Purdue Research Foundation to the Signal Corps, August 1952 (unpublished).

33 Willardson, Harman and Beer, Phys. Rev. 96, 1512 (1954).

34 H. Ehrenreich and A. W. Overhauser, Bull. Am. Phys. Soc. 30, No. 2, p 10 (1955).

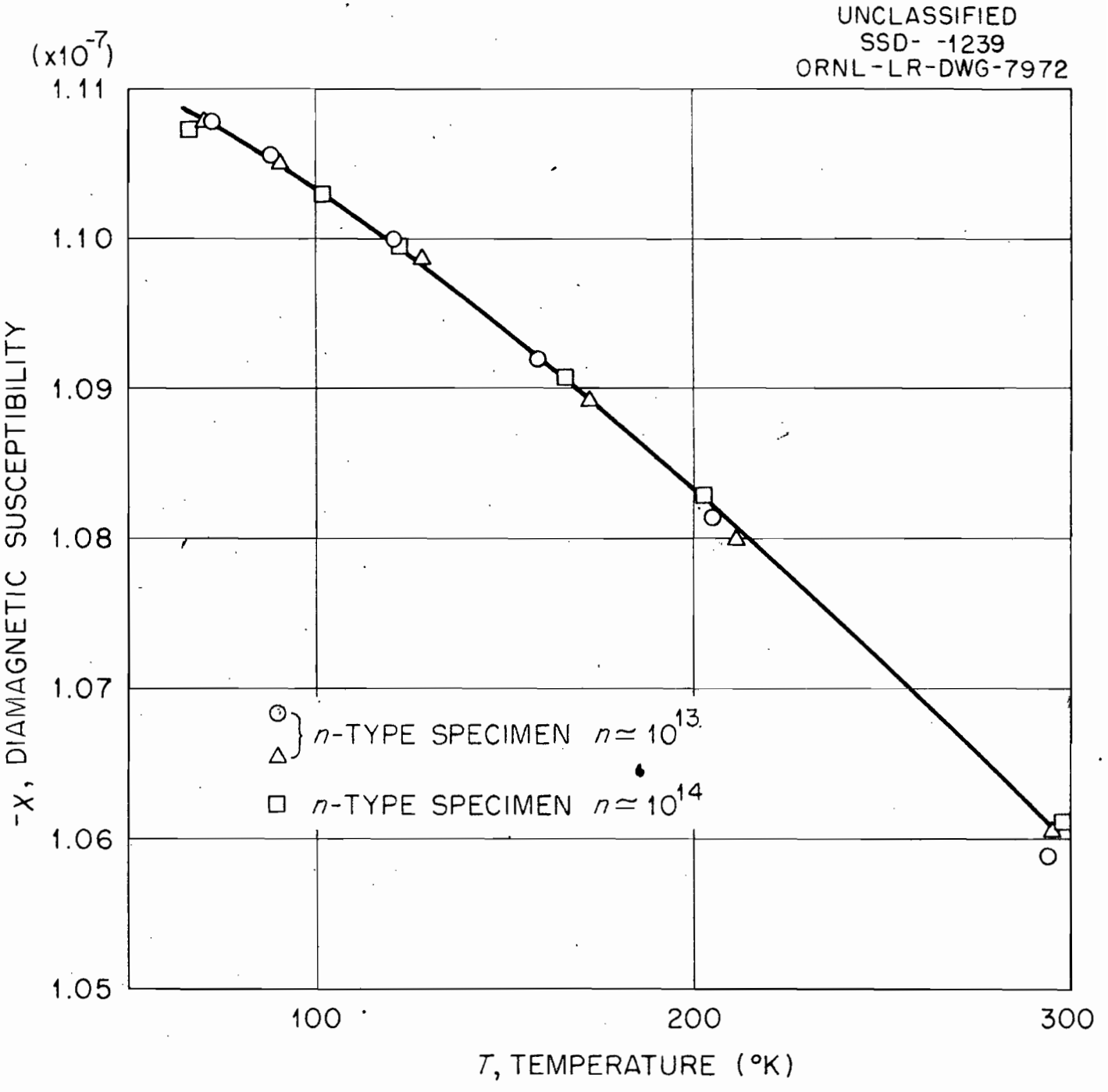
UNCLASSIFIED
SSD- -1239
ORNL-LR-DWG-7972
(x10^-7)
1.11
1.10
1.09
1.08
1.07
1.06
1.05
-χ, DIAMAGNETIC SUSCEPTIBILITY
n-TYPE SPECIMEN n ≃ 10^13
n-TYPE SPECIMEN n ≃ 10^14
100
200
300
T, TEMPERATURE (°K)

UNCLASSIFIED
SSD- -1238
ORNL-LR-DWG-7971

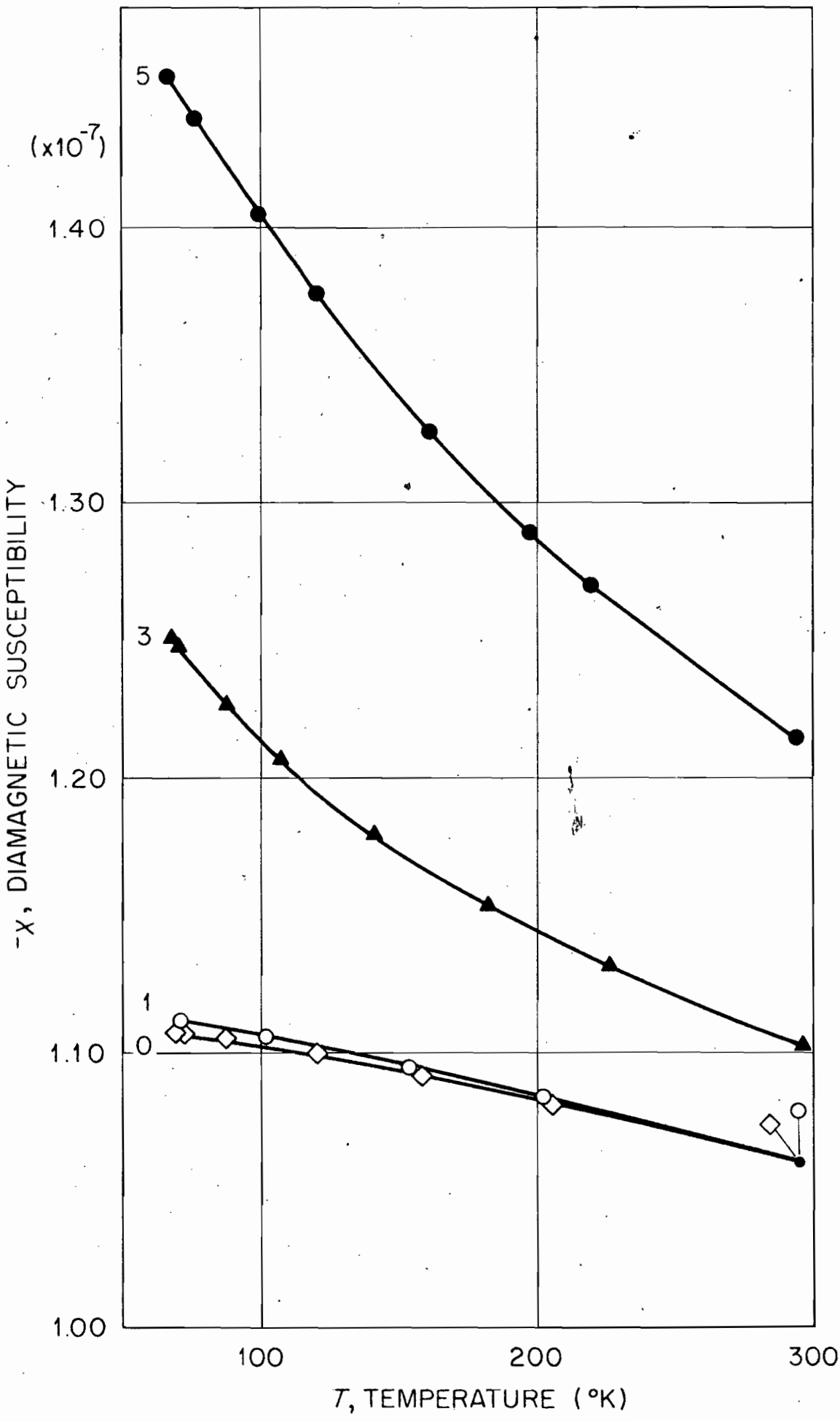

UNCLASSIFIED
SSD- -1237
ORNL-LR-DWG-7970

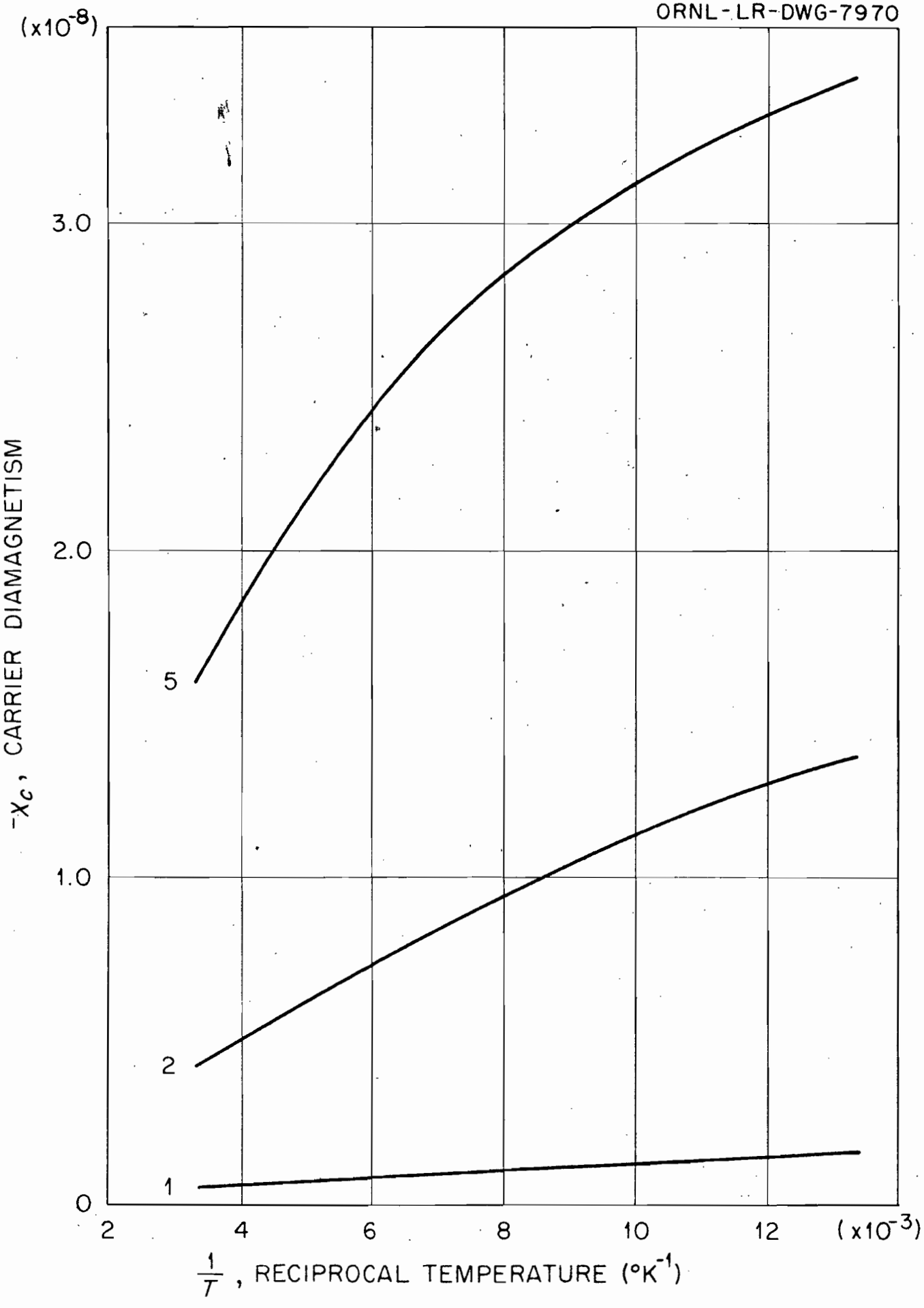

UNCLASSIFIED
SSD- -1234
ORNL-LR-DWG-7967

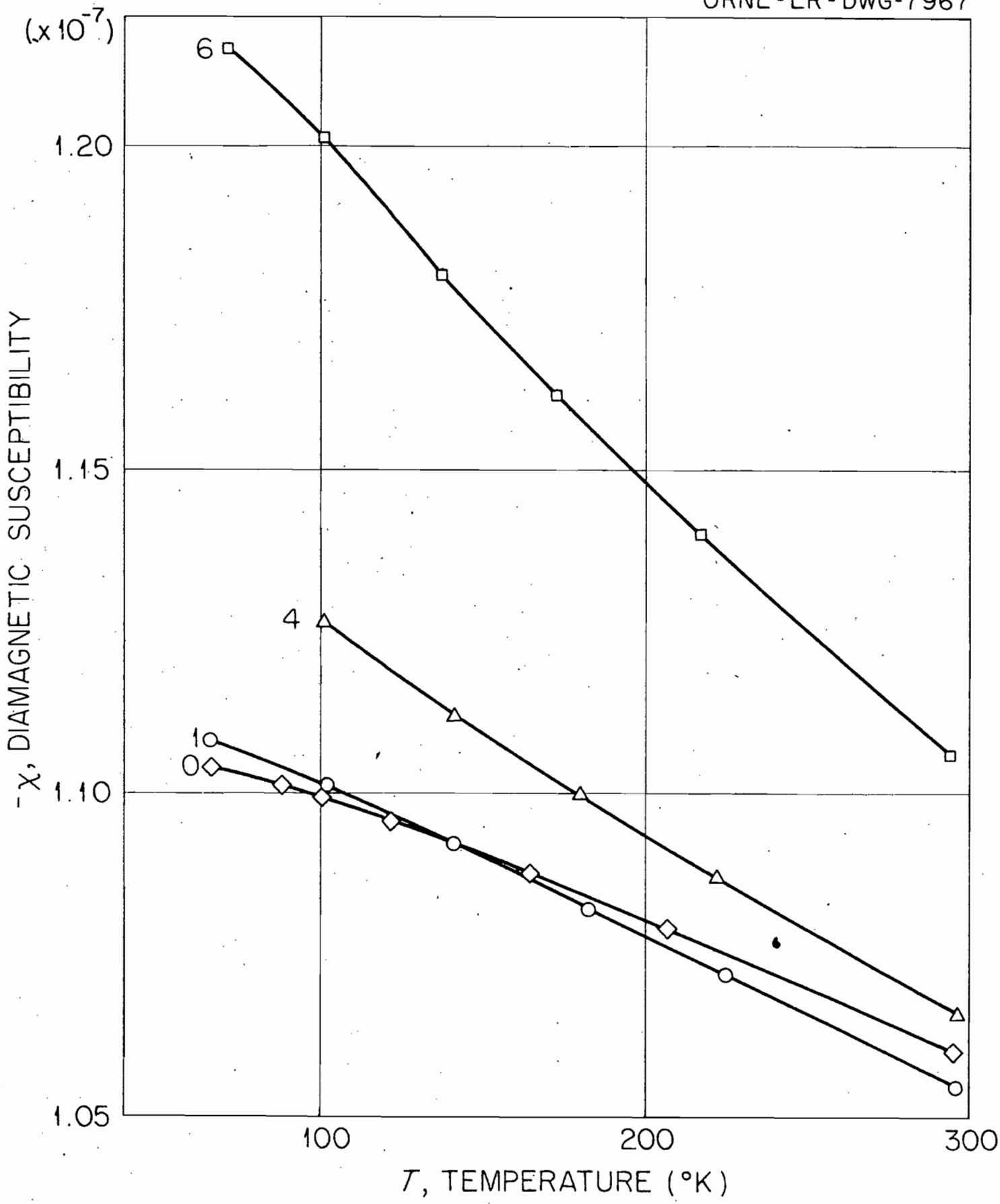

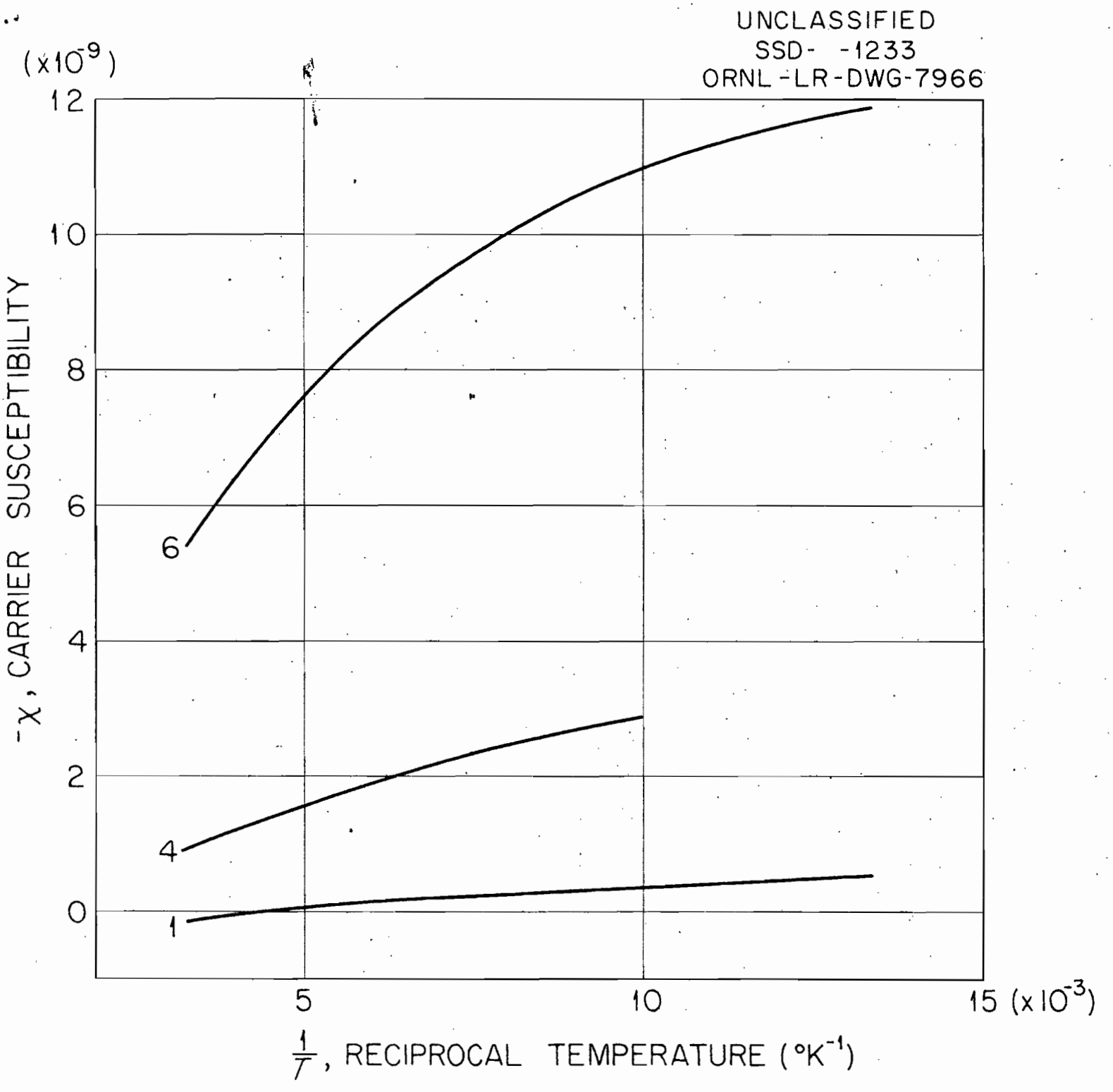
UNCLASSIFIED
SSD- -1233
ORNL-LR-DWG-7966
(x10^-9)
12
10
8
6
4
2
0
-χ, CARRIER SUSCEPTIBILITY
6
4
1
5
10
15 (x10^-3)
1/T, RECIPROCAL TEMPERATURE (°K^-1)

UNCLASSIFIED
SSD- -1236
ORNL-LR-DWG-7969

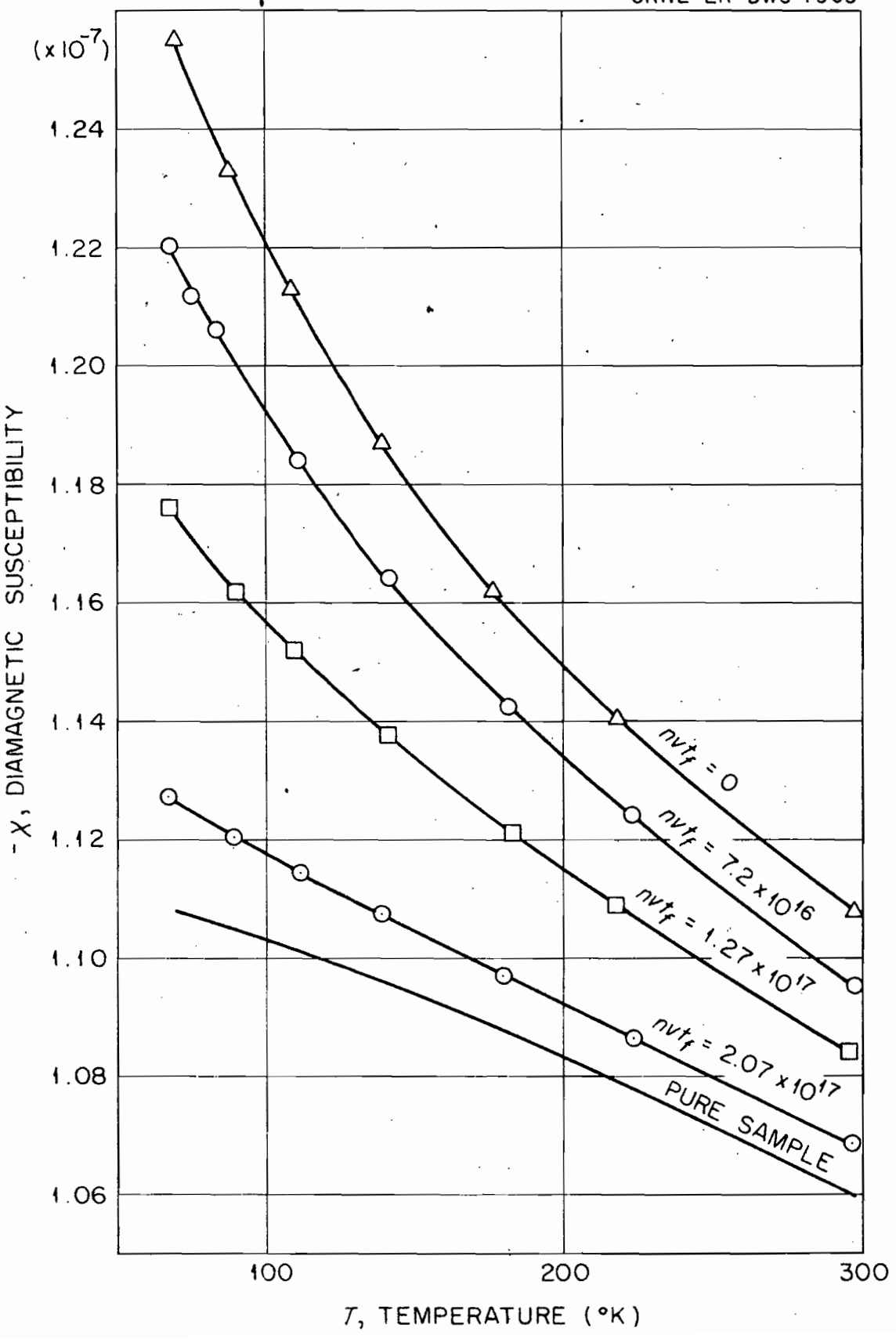

UNCLASSIFIED
SSD- -1235
ORNL-LR-DWG-7968

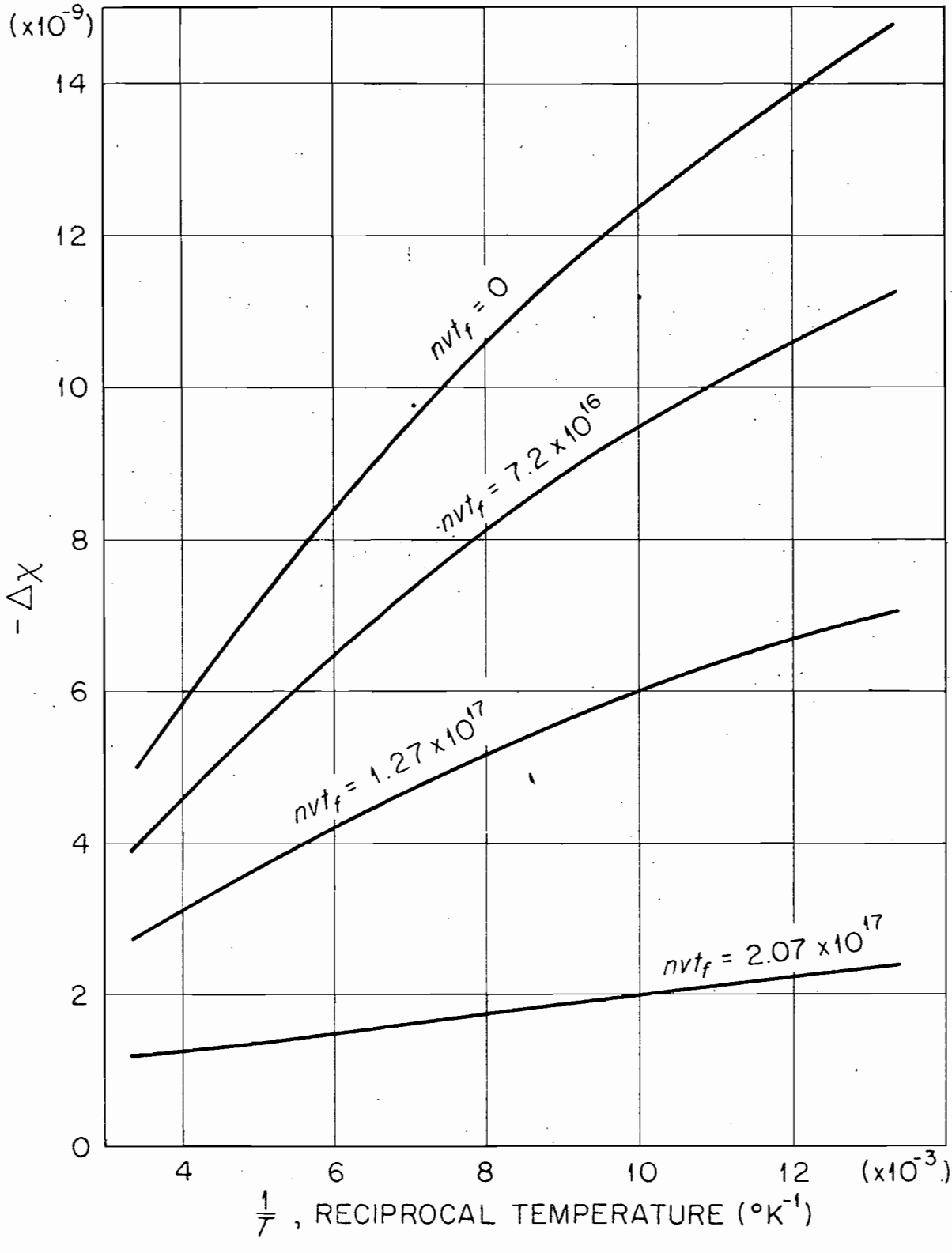

UNCLASSIFIED
SSD- -1240
ORNL-LR-DWG-7973

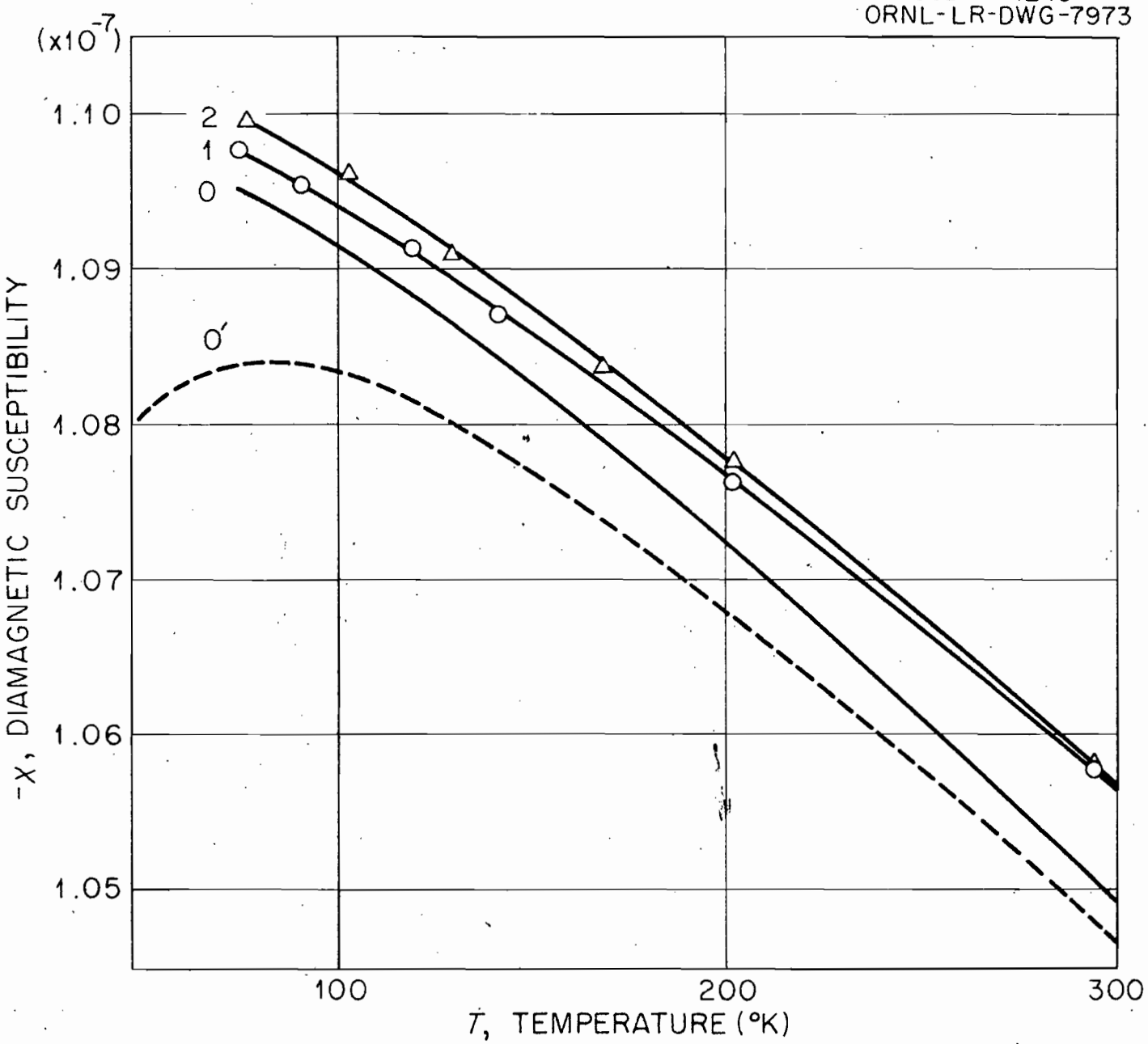
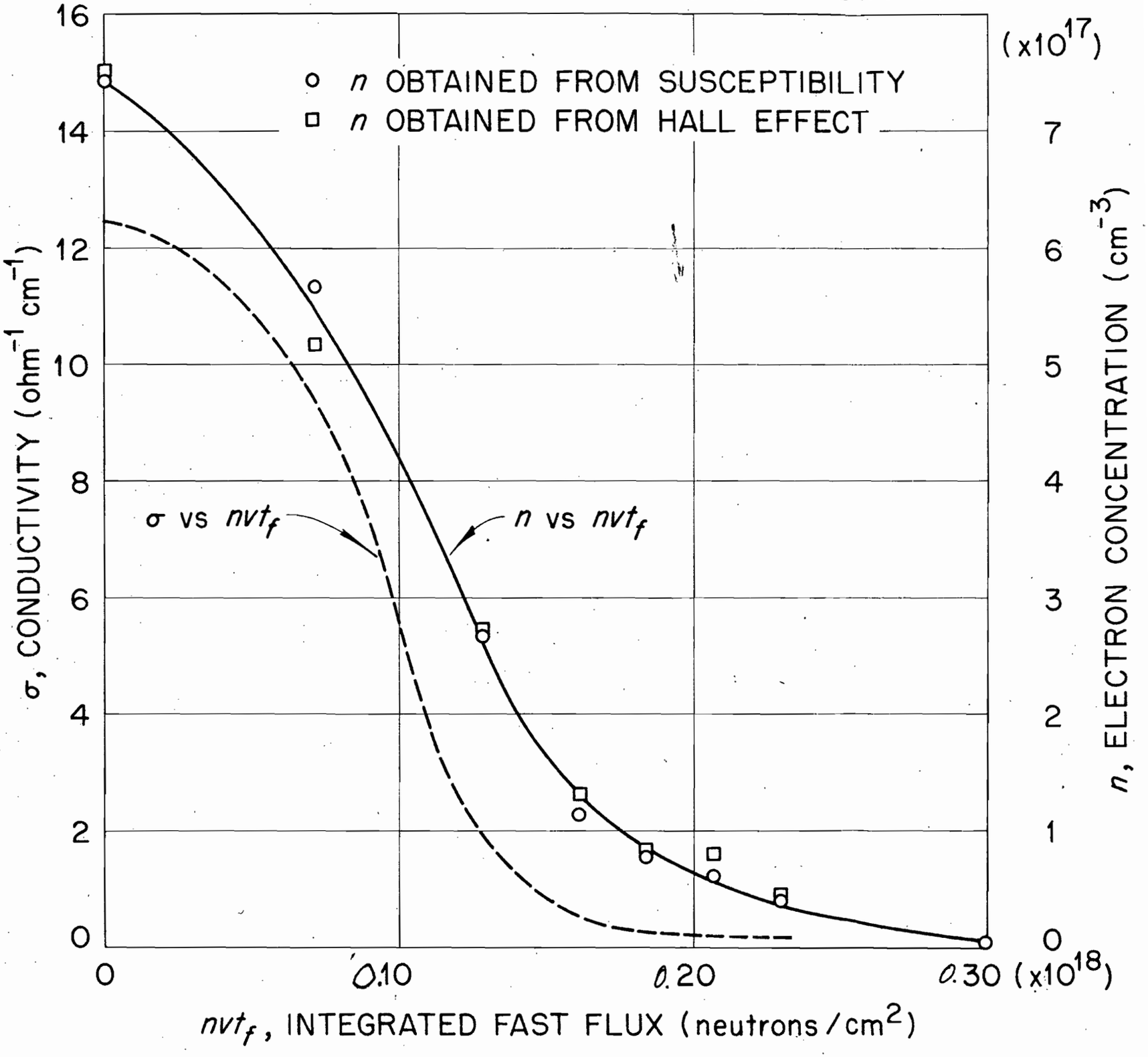
UNCLASSIFIED
SSD- -1232
ORNL-LR-DWG-7965